Dual synchronization of chaos in Colpitts electronic oscillators and its applications for communications

A. Uchida, M. Kawano, and S. Yoshimori
Department of Electronics and Computer Systems, Takushoku University, 815-1 Tatemachi, Hachioji, Tokyo 193-0985, Japan
(Received 29 July 2002; revised manuscript received 27 May 2003; published 20 November 2003)

We demonstrate the dual synchronization of chaos in two pairs of one-way coupled Colpitts electronic oscillators by both experiment and numerical simulation. We use the cross coupling method, where the difference in voltage between the sum of two master oscillators and one slave oscillator is injected into the other slave oscillator as an electrical current, for dual synchronization of chaos. We have investigated the regions for achieving dual synchronization of chaos when one of the internal parameters is mismatched between the master and slave oscillators. We numerically obtain a similar curve for the accuracy of synchronization to that obtained from our experiments. A communication scheme using dual synchronization of chaos is also proposed and demonstrated.

DOI: 10.1103/PhysRevE.68.056207 PACS number(s): 05.45.Xt, 05.45.Vx

I. INTRODUCTION

Synchronization of chaos in electronic circuits has attracted increasing interest for the applications of secure communications [1,2] and spread spectrum communications [3]. Synchronization of chaos can be used for sharing the identical chaos in a transmitter and a receiver as a cryptographical code. Many studies on synchronization of chaos have been reported in one-way coupled chaotic systems [1,2]. However, since the configuration of synchronization is limited to a single pair of one-way coupled oscillators, this method cannot be applied for multiuser communication systems [4]. From the nonlinear dynamic point of view, synchronization of chaos in multiple pairs of one-way coupled oscillators is a very interesting topic, which is related to the identification of chaos from mixed chaotic wave forms.

The technique of multiplexing is a very important issue for high capacity communications [4]. Multiplexing chaos using synchronization has been reported in a simple map and electronic circuit model by Tsimring and Sushchik [5]. Dual synchronization of chaos for synchronizing two different pairs of chaotic maps and delay-differential equations has also been investigated by Liu and Davis [6]. To synchronize each pair of chaotic systems, all the parameter settings must be identical between the transmitter and the receiver, whereas they must be slightly shifted between different pairs of chaotic systems. Although it has been shown theoretically in Refs. [5,6] that it is possible to synchronize each pair of multiplexed chaotic oscillators, these multiplexing synchronization methods have not been experimentally confirmed. It is important to investigate synchronization of multiplexing chaos in electronic circuits by experiment.

Chaotic electronic oscillators for communications require specific characteristics such as broadband, security, and low interference code generation. One of the good candidates of chaotic electronic circuits for communications is the Colpitts oscillator, which has a simple configuration consisting of a single bipolar junction transistor and some passive elements. Nonlinear dynamics and chaotic phenomena in Colpitts oscillators have been intensively investigated and rich dynamic behavior has been reported [7–16]. From the communication applications point of view, broadband chaotic oscillations over 3 GHz have been demonstrated by using two-stage Colpitts oscillators [17]. Synchronization of chaos in one pair of Colpitts oscillators has also been demonstrated [18–21].

In this paper, we demonstrate the dual synchronization of chaos in two pairs of one-way coupled Colpitts oscillators by both experiment and numerical simulation. We use cross coupling for dual synchronization. The degree of synchronization is quantitatively evaluated by using the variance of correlation plots from the best-fit linear relationship. We investigate the parameter regions for achieving dual synchronization when one of the internal parameters is mismatched between the master and slave oscillators, and clarify the tolerance to mismatch parameters for synchronization. We also demonstrate a communication scheme by using dual synchronization of chaos.

II. EXPERIMENT

A. Experimental setup

We show a block diagram for dual synchronization using Colpitts oscillators in Fig. 1. Two of the Colpitts oscillators are used as master oscillators, which we refer to as ''M1'' for master 1 and ''M2'' for master 2. The other two oscillators are used as slave oscillators (''S1'' for slave oscillator 1 and ''S2'' for slave oscillator 2). The voltages in two master oscillators are combined as a transmission signal, and the signal is transmitted to the two slave oscillators. In front of the slave oscillators, the transmission signal is subtracted by the voltage of the other slave oscillators, i.e., the injection signal is written as $V_{m1}+V_{m2}-V_{s2}$ for the S1 oscillator, and $V_{m1}+V_{m2}-V_{s1}$ for the S2 oscillator. For S1, the injection signal is equal to M1 under the condition of synchronization between M2 and S2, because the S2 component cancels the M2 component from the mixed signal M1+M2. This is equivalent to a one-pair system. When synchronization manifolds for the pair of M1 and S1, and the pair of M2 and S2 are stable, dual synchronization can be achieved.

Figure 2 shows the four Colpitts oscillators used in our experiments. Each Colpitts circuit consists of a single bipolar

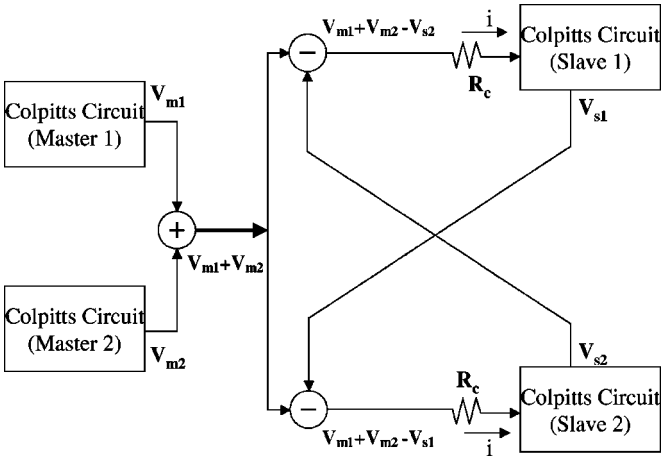

FIG. 1. Block diagram for dual synchronization of chaos using four Colpitts electronic oscillators.

junction transistor (2SC1740, Rohm Co. LD., cutoff frequency of 180 MHz) which is biased in the active region by means of V_{ee}, R_{ee}, and V_{cc}. The oscillator components consist of an inductor L with series resistance R_l, and two capacitors C_1 and C_2. The voltages of the collector-emitter junction and the base-emitter junction are denoted as V_{ce} and V_{be}, respectively. The additional subscripts m1,m2, s1, s2 of the parameters indicate the master 1, master 2, slave 1, and slave 2 oscillators, respectively. Two of the Colpitts oscillators are combined through two voltage followers and an inverting adder circuit using operational amplifiers (LM6361N). The combined signal is injected into two subtractor circuits in order to subtract a voltage of S1 and S2 in front of S2 and S1 circuit, respectively. Each electrical current is injected into the collector of each slave transistor through a coupling resistor R_c as a synchronization signal. The current is proportional to the difference between the voltages before and after the coupling resistor. The amount of the current can be changed by R_c. The parameters used in our experiments are summarized in Table I. Note that the resistors R_l are identical for the pair of M1 and S1 (referred to as "M1-S1") (36.0 Ω) and the pair of M2 and S2 (referred to as "M2-S2") (24.0 Ω), but are different in the pairs of M1-S2 and M2-S1 in order to achieve dual synchronization. The other parameters are set to be as identical as possible. In this condition, since the chaotic attractors are identical for M1-S1 and M2-S2, dual synchronization can be achieved. Although we attempt to match the values of all the parameters between the master and slave oscillators for accurate synchronization, some errors in parameter matching exist in experiment. We measure temporal wave forms of V_{be} in the four oscillators by using a digital oscilloscope (Sony-Tektronix: TDS-420A).

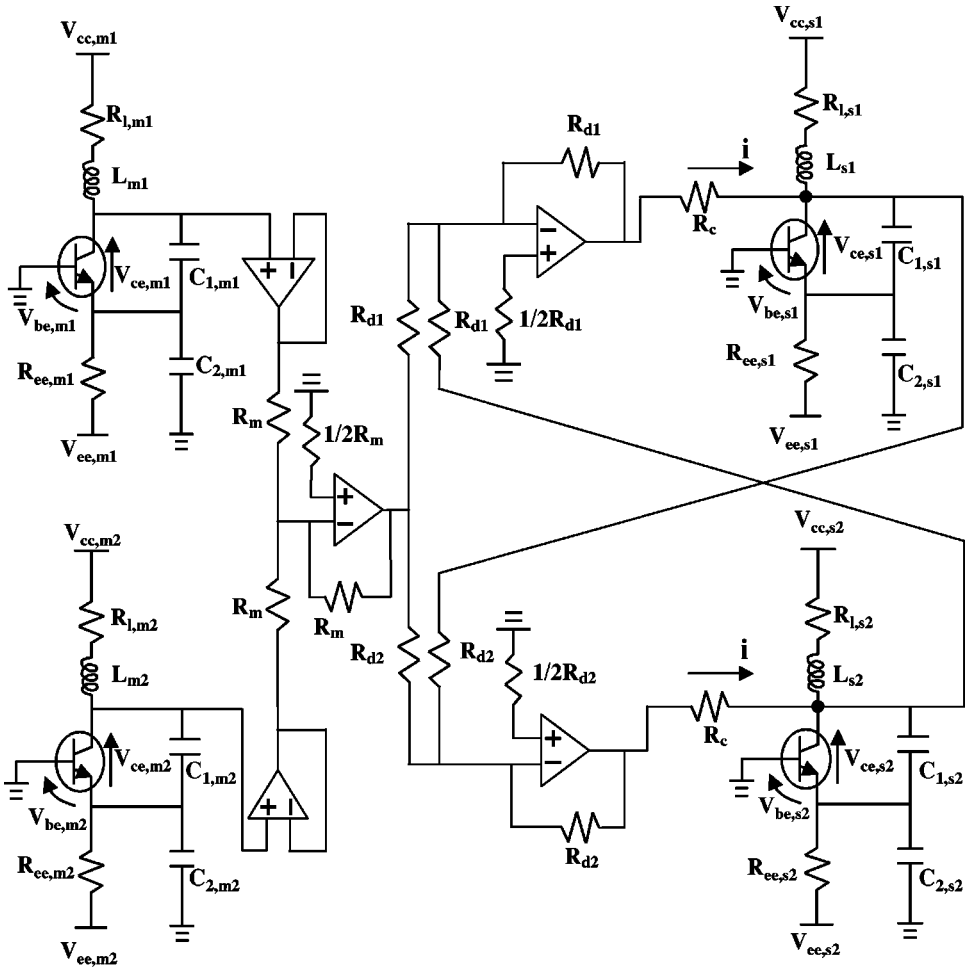

FIG. 2. Schematics of our experimental setup for dual synchronization of chaos in four Colpitts electronic oscillators. The parameters are shown in Table I. $R_m = R_{d1} = R_{d2} = 9.1\ \mathrm{k}\Omega$.

TABLE I. Parameter values for the four Colpitts oscillators obtained from our experiments.

Parameters	Master 1	Master 2	Slave 1	Slave 2
C_1 [nF]	57.44	57.00	57.52	56.90
C_2 [nF]	57.55	57.82	57.66	57.58
L [μH]	99.44	100.30	99.56	99.62
R_1 [Ω]	36.0	24.0	36.0	24.0
R_{ee} [Ω]	430	430	430	430
V_{cc} [V]	5.0	5.0	5.0	5.0
V_{ee} [V]	−5.0	−5.0	−5.0	−5.0
R_{on} [Ω]	376	376	375	351
h_{fe} ($=\beta_f$)	238	244	228	220
V_{th} [V]	0.678	0.679	0.674	0.679
R_c [Ω]		20.0		

B. Experimental results of dual synchronization

Without coupling between the master and slave oscillators, chaotic oscillations are observed through some bifurcation processes in all the circuits. These dynamics are considered as deterministic chaos, as reported in Refs. [8–10]. For dual synchronization, the coupling resistors R_c are set to 20.0 Ω. Figure 3 shows temporal wave forms of V_{be} and their correlation plots of the corresponding pairs of M1-S1 and M2-S2, and of different pairs of M1-S2 and M2-S1. Synchronization of chaotic oscillations is independently achieved for the corresponding pairs, M1-S1 and M2-S2, as shown in Figs. 3(a)–3(d). A linear correlation is observed as shown in Figs. 3(b) and 3(d). Conversely, synchronization of chaos is not achieved for the other pairs of M1-S2 and M2-S1, as shown in Figs. 3(e)–3(h). We calculate the cross correlation between the temporal wave forms of the master and slave oscillators, $C_{V_{m,i},V_{s,j}}=\langle \Delta V_{m,i}\Delta V_{s,j}\rangle/(\sigma_{V_{m,i}}\sigma_{V_{s,j}})$, where $\Delta V_{m,i}$ and $\Delta V_{s,j}$ are the deviations of the Master-i and Slave-j voltages from the mean values and $\sigma_{V_{m,i}}$ and $\sigma_{V_{s,j}}$ are the standard deviations of the Master-i and Slave-j voltages. The angle brackets denote time averaging. The cross correlations between the Master-i and Slave-j voltages are estimated as 0.998 for Fig. 3(b), 0.998 for Fig. 3(d), 0.084 for Fig. 3(f), and 0.033 for Fig. 3(h). Thus, we have experimentally achieved dual synchronization of chaos between M1 and S1, and between M2 and S2, respectively, in one-way coupled Colpitts oscillators.

Figure 4 shows the transmission signal of M1+M2 and the output of S1. Only the oscillation of M1 is reproduced in the S1 oscillator from the combined signal of M1+M2, which indicates that separate synchronization has been achieved in our systems. No linear correlation is observed between the transmission signal and the synchronized S1 signal as shown in Fig. 4(b).

To evaluate the quantitative accuracy of chaos synchronization, variance σ^2 of the normalized correlation plot from the best-fit linear relationship is defined as follows [22,23]:

$$\sigma^2=\frac{1}{N}\sum_{i}^{N}(V_{\mathrm{m,i}}-V_{\mathrm{s,i}})^2, \tag{2.1}$$

where N is the total number of samples of the temporal wave forms. $V_{\mathrm{m,i}}$ and $V_{\mathrm{s,i}}$ are the normalized voltages of the master and slave oscillators at the ith sampling point. Smaller variance σ^2 indicates higher accuracy of chaos synchronization. In the cases of Figs. 3(b), 3(d), 3(f), and 3(h), the variances σ^2 are calculated as 3.6×10^{-4}, 3.0×10^{-4}, 1.0×10^{1}, and 6.6×10^{1}, respectively.

We investigate the characteristics of dual synchronization when the values of the coupling resistors R_c are varied. Figure 5 shows the accuracy of synchronization for the pair of M1-S1 as a function of R_c. The accuracy of synchronization gradually decreases with decrease of R_c from 50 Ω. The best accuracy is obtained at R_c of 21 Ω. We define a synchronization region where the variance σ^2 is greater than ten times the minimum σ^2 when one of the parameters is changed. For example, since the minimum accuracy is 5.3×10^{-4} in Fig. 5, we define the synchronization range where the accuracy is less than 5.3×10^{-3}, which is ten times of the minimum accuracy of 5.3×10^{-4}. The synchronization of chaos can be achieved in the range of R_c from 10 Ω to 36 Ω. Hence, we found that there is an optimum value of R_c for achieving accurate synchronization of chaos.

We quantitatively investigate chaos-synchronization regions against parameter mismatch for some parameters in the two pairs of Colpitts oscillators. One of the parameters of M1 is fixed and the corresponding parameter of S1 is shifted. Other parameters of M1 and S1 are set to be as identical as possible, although there still exist some errors in our experimental systems. All the parameters of the other pair of M2-S2 are also fixed. Figure 6 shows the accuracy of synchronization for the pair of M1-S1 (variance σ^2) as a function of parameter mismatch of (a) $R_{\mathrm{l,s1}}$ and (b) $R_{\mathrm{ee,s1}}$. The best accuracy is obtained with matched parameters for both the figures, although the shape of the curves is different in Figs. 6(a) and 6(b). This demonstrates that mismatched parameters reduce the accuracy of synchronization. We estimate the synchronization ranges for the variable parameters by using the criteria of σ^2 greater than ten times the minimum σ^2 as follows: (a) $-8.3\%<R_{\mathrm{l,s1}}<+12.0\%$ and (b) $-2.3\%<R_{\mathrm{ee,s1}}<+18.6\%$. The region for achieving synchronization is strongly dependent upon each parameter.

We found that synchronization can be switched between the two pairs of oscillators when the resistor values of R_l are set to be equal for all the oscillators. When all the parameters are close enough to each other, the S1 oscillator can be synchronized with either M1 or M2, depending on the initial conditions. In this case, since the structure of the attractors for M1 and M2 are similar, the synchronization manifold is strongly dependent on the initial condition. It is important for the achievement of dual synchronization to set parameters significantly different between the pairs of M1-S1 and M2-S2.

III. NUMERICAL CALCULATIONS

A. Model

To describe the dynamics of Colpitts oscillators, we use a model proposed in Ref. [7]. We modify the model for two

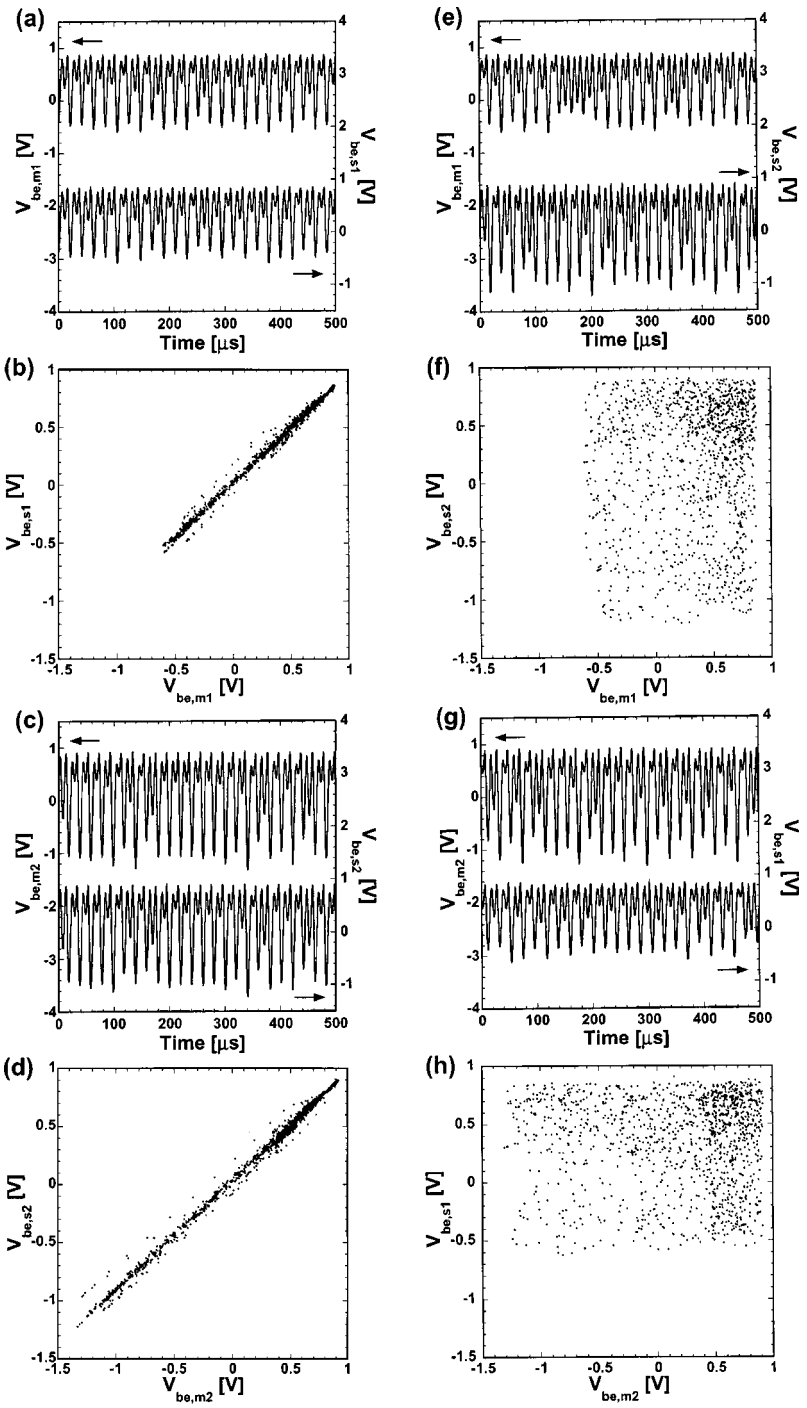

FIG. 3. Temporal wave forms and their correlation plots for the pair of M1-S1 [(a),(b)], M2-S2 [(c),(d)], M1-S2 [(e),(f)], and M2-S1 [(g),(h)].

pairs of one-way coupled Colpitts oscillators. The four circuits can be described by autonomous state equations as follows:

Master oscillator 1:

$$C_{1,\mathrm{m1}}\frac{dV_{\mathrm{ce,m1}}}{dt}=I_{\mathrm{l,m1}}-I_{\mathrm{c,m1}}, \tag{3.1}$$

$$C_{2,\mathrm{m1}}\frac{dV_{\mathrm{be,m1}}}{dt}=-\frac{V_{\mathrm{ee,m1}}+V_{\mathrm{be,m1}}}{R_{\mathrm{ee,m1}}}-I_{\mathrm{b,m1}}-I_{\mathrm{l,m1}} \tag{3.2}$$

$$L_{\mathrm{m1}}\frac{dI_{\mathrm{l,m1}}}{dt}=V_{\mathrm{cc,m1}}-V_{\mathrm{ce,m1}}+V_{\mathrm{be,m1}}-I_{\mathrm{l,m1}}R_{\mathrm{l,m1}}. \tag{3.3}$$

Master oscillator 2:

$$C_{1,\mathrm{m2}}\frac{dV_{\mathrm{ce,m2}}}{dt}=I_{\mathrm{l,m2}}-I_{\mathrm{c,m2}}, \tag{3.4}$$

$$C_{2,\mathrm{m2}}\frac{dV_{\mathrm{be,m2}}}{dt}=-\frac{V_{\mathrm{ee,m2}}+V_{\mathrm{be,m2}}}{R_{\mathrm{ee,m2}}}-I_{\mathrm{b,m2}}-I_{\mathrm{l,m2}}, \tag{3.5}$$

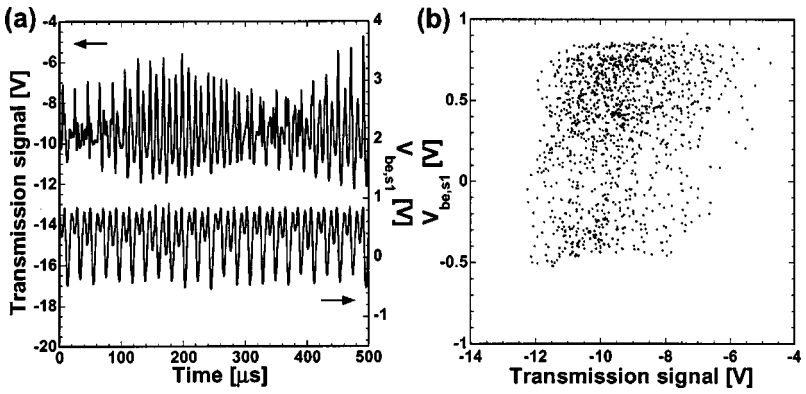

FIG. 4. (a) Temporal wave forms and (b) their correlation plots for the transmission signal of the sum of Master 1 and Master 2 and the output of Slave 1.

$$L_{m2}\frac{dI_{l,m2}}{dt}=V_{cc,m2}-V_{ce,m2}+V_{be,m2}-I_{l,m2}R_{l,m2}. \quad (3.6)$$

Slave oscillator 1:

$$C_{1,s1}\frac{dV_{ce,s1}}{dt}=I_{l,s1}-I_{c,s1}+\frac{1}{R_c}\{(V_{ce,m1}-V_{be,m1}) +(V_{ce,m2}-V_{be,m2})-(V_{ce,s2}-V_{be,s2}) -(V_{ce,s1}-V_{be,s1})\}, \quad (3.7)$$

$$C_{2,s1}\frac{dV_{be,s1}}{dt}=-\frac{V_{ee,s1}+V_{be,s1}}{R_{ee,s1}}-I_{b,s1}-I_{l,s1} -\frac{1}{R_c}\{(V_{ce,m1}-V_{be,m1})+(V_{ce,m2}-V_{be,m2}) -(V_{ce,s2}-V_{be,s2})-(V_{ce,s1}-V_{be,s1})\}, \quad (3.8)$$

$$L_{s1}\frac{dI_{l,s1}}{dt}=V_{cc,s1}-V_{ce,s1}+V_{be,s1}-I_{l,s1}R_{l,s1}. \quad (3.9)$$

Slave oscillator 2:

$$C_{1,s2}\frac{dV_{ce,s2}}{dt}=I_{l,s2}-I_{c,s2}+\frac{1}{R_c}\{(V_{ce,m1}-V_{be,m1}) +(V_{ce,m2}-V_{be,m2})-(V_{ce,s1}-V_{be,s1}) -(V_{ce,s2}-V_{be,s2})\}, \quad (3.10)$$

$$C_{2,s2}\frac{dV_{be,s2}}{dt}=-\frac{V_{ee,s2}+V_{be,s2}}{R_{ee,s2}}-I_{b,s2}-I_{l,s2} -\frac{1}{R_c}\{(V_{ce,m1}-V_{be,m1})+(V_{ce,m2}-V_{be,m2}) -(V_{ce,s1}-V_{be,s1})-(V_{ce,s2}-V_{be,s2})\}, \quad (3.11)$$

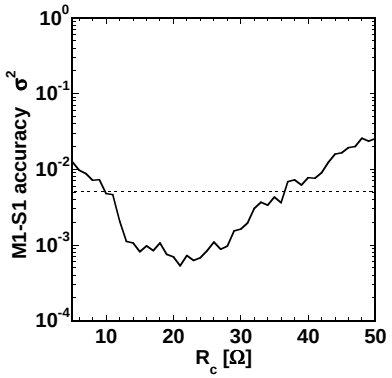

FIG. 5. Accuracy of dual synchronization of chaos for the pair of M1-S1 as a function of R_c. The dotted line indicates the threshold of synchronization.

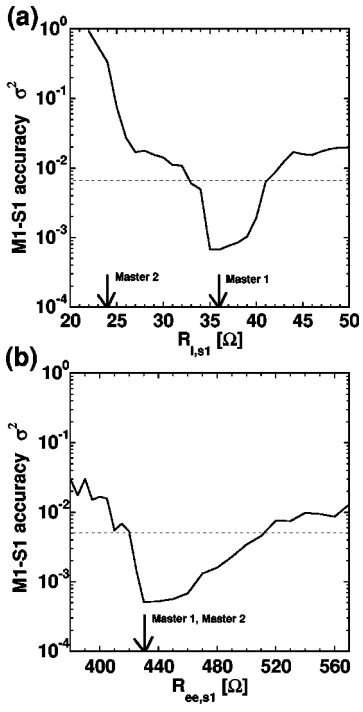

FIG. 6. Accuracy of dual synchronization of chaos for the pair of M1-S1 as functions of (a) $R_{l,s1}$ and (b) $R_{ee,s1}$. The dotted line indicates the threshold of synchronization. The vertical arrows indicate the parameter values of M1 and M2 for R_l and R_{ee}.

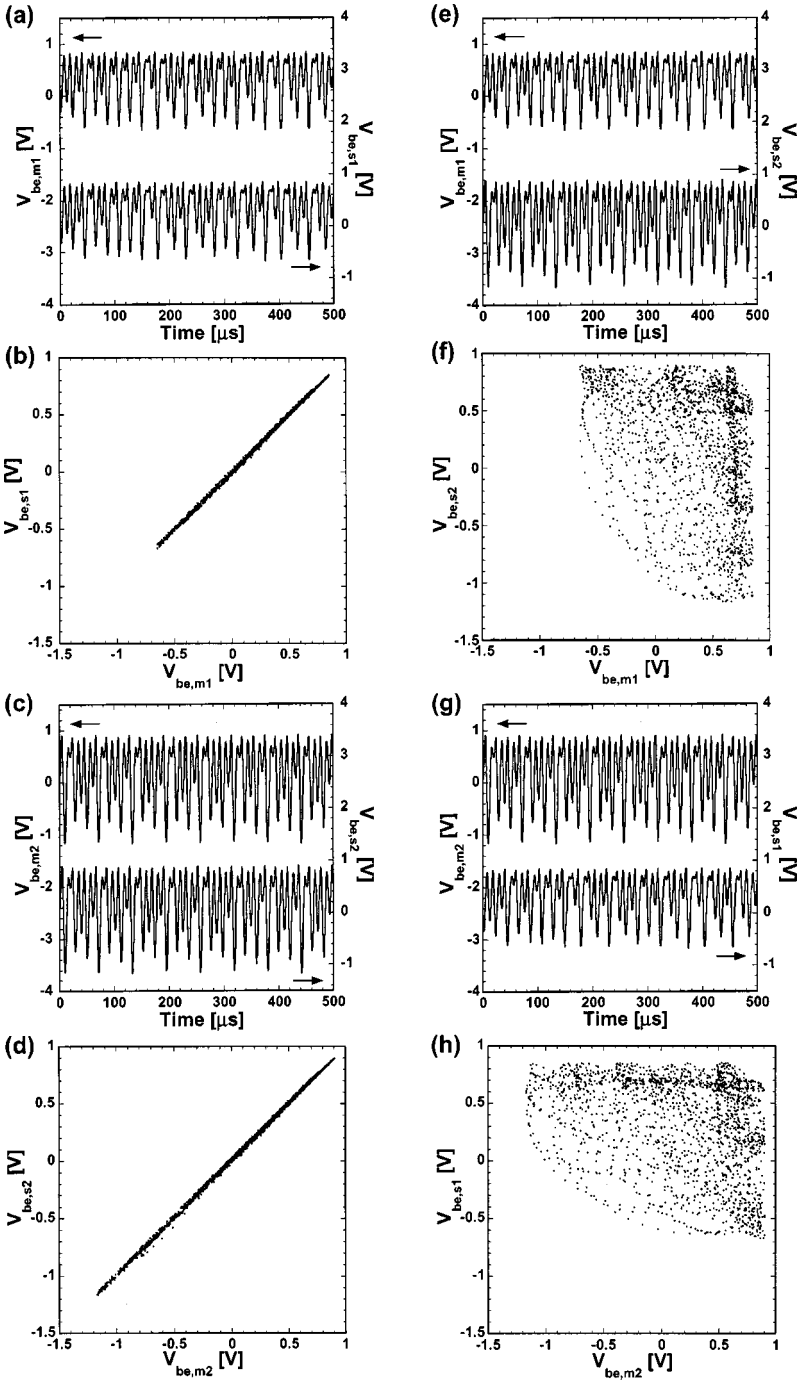

FIG. 7. Numerical results showing temporal waveforms and their correlation plots for the pair of M1-S1 [(a),(b)], M2-S2 [(c),(d)], M1-S2 [(e),(f)], and M2-S1 [(g),(h)].

$$L_{s2}\frac{dI_{l,s2}}{dt}=V_{cc,s2}-V_{ce,s2}+V_{be,s2}-I_{l,s2}R_{l,s2}. \quad (3.12)$$

The bipolar junction transistor operates in two regions: forward active and cutoff. We thus model the transistor as a two-segment piecewise-linear voltage-controlled resistor and a linear current-controlled current source. The base current I_b and the collector current I_c are described as follows [7]:

$$I_b=\begin{cases}0, & V_{be}\leqslant V_{th}\\ \dfrac{V_{be}-V_{th}}{R_{on}}, & V_{be}>V_{th},\end{cases} \quad (3.13)$$

$$I_c=\beta_f I_b, \quad (3.14)$$

where V_{th} is the threshold voltage, R_{on} is the small-signal on-resistance of the base-emitter junction, and β_f $(=h_{fe})$ is the forward current gain of the device. We numerically integrate Eqs. (3.1)–(3.12) by using the fourth-order Runge-Kutta-Gill method.

B. Numerical results

For a practical situation, we include parameter mismatch between the master and slave oscillators as in the case of our experiments. We use the experimental parameters shown in

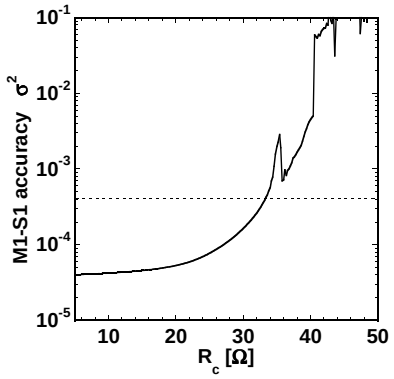

FIG. 8. Numerical results showing accuracy of dual synchronization of chaos for the pair of M1-S1 as a function of R_c. The dotted line indicates the threshold of synchronization.

Table I for our calculations, except $R_{l,m2}=R_{l,s2}=25.5\ \Omega$, $h_{fe,m2}=206.5$, and $h_{fe,s2}=195.0$. We adjust the values of $R_{l,m2}$, $R_{l,s2}$, $h_{fe,m2}$, and $h_{fe,s2}$ so that we can obtain the same dynamical region of chaos and bifurcation diagram between experiments and calculations. For dual synchronization, the resistors of M1 and S1 are set to be identical at $R_{l,m1}=R_{l,s1}=36.0\ \Omega$, whereas the resistors of M2 and S2 are identical at $R_{l,m2}=R_{l,s2}=25.5\ \Omega$.

Figure 7 shows temporal wave forms of V_{be} and their correlation plots between one of the master oscillators and one of the slave oscillators with the coupling at $R_c=20.0\ \Omega$. Synchronization of chaotic oscillations is achieved for the pairs of M1-S1 and M2-S2, as shown in Figs. 7(a)–7(d). We have confirmed the variables of V_{ce} and I_l in Eqs. (3.1)–(3.12) are also synchronized between the two corresponding oscillators. Conversely, the different pairs of oscillators for M1-S2 and M2-S1 are not synchronized to each other in Figs. 7(e)–7(h). These numerical results agree well with our experimental results shown in Fig. 3.

To investigate the characteristics of parameter dependence, we change the coupling resistance R_c. We use the variance σ^2 to evaluate the accuracy of synchronization. Figure 8 shows the accuracy of synchronization as a function of R_c. The accuracy is gradually improved (σ^2 decreases) as R_c is decreased. Synchronization is achieved in the range of R_c less than 32 Ω except $R_c=0$. The shape of the curves is similar to that obtained by experiment as shown in Fig. 5, except at the region of small values of R_c. We consider that the discrepancy between Figs. 5 and 8 derives from the huge amount of electronic current into the transistors in the Slave

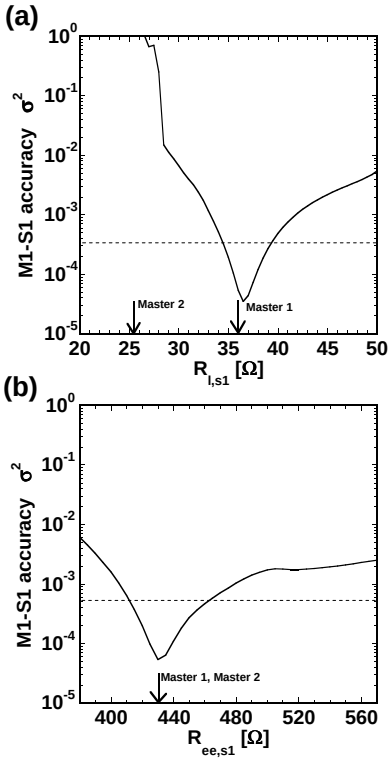

FIG. 9. Numerical results showing accuracy of dual synchronization of chaos for the pair of M1-S1 as functions of (a) $R_{l,s1}$ and (b) $R_{ee,s1}$. The dotted line indicates the threshold of synchronization. The vertical arrows indicate the parameter values of M1 and M2 for R_l and R_{ee}.

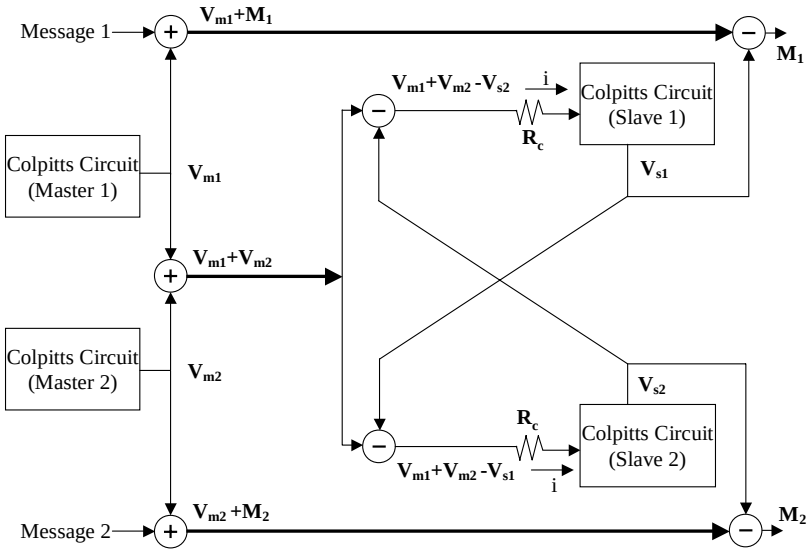

FIG. 10. Block diagram for our communication scheme using dual synchronization of chaos. The bold lines correspond to the transmission channels.

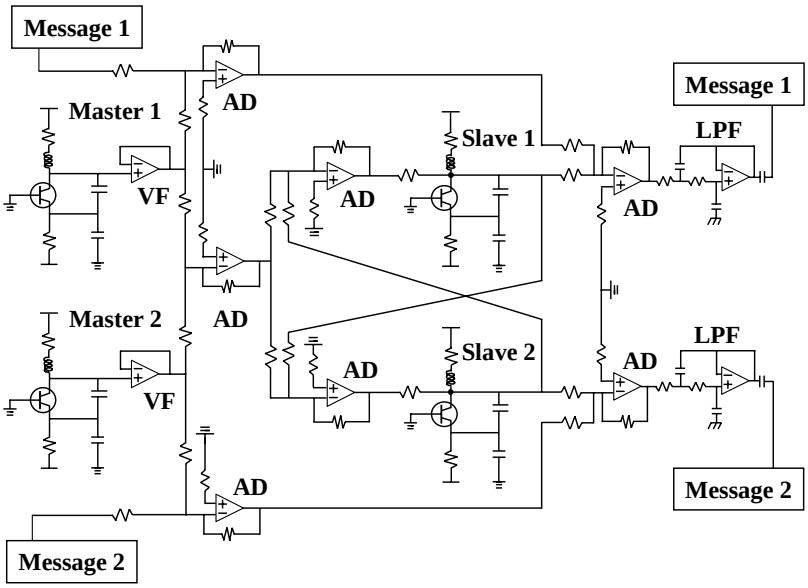

FIG. 11. Schematics of our experimental setup for our communication scheme using dual synchronization of chaos. AD: inverting adder circuit, LPF: low pass filter, and VF: voltage follower.

oscillators at small R_c. The increase of electronic current into the transistors with decreasing R_c results in the change of nonlinearity of the transistors, which is not described as a piecewise linear voltage-current (V-I) curve in our model. Therefore, we cannot observe good synchronization at small R_c in the experiment shown in Fig. 5, even though the model suggests the synchronization at this region as shown in Fig. 8.

We also investigate chaos-synchronization regions against parameter mismatch for different parameters in the two pairs of the Colpitts oscillators. One of the parameters of M1 is fixed and the corresponding parameter of S1 is shifted. Other parameters are set to be as identical as possible, shown in Table 1. Figure 9 shows the accuracy of synchronization (variance σ^2) as a function of parameter mismatch of (a) $R_{l,s1}$ and (b) $R_{ee,s1}$. The accuracy is gradually changed and the best accuracy is obtained at the parameter matching condition between M1 and S1. The synchronization range for each parameter can be obtained as follows: (a) $-5.5\% < R_{l,s1} < +8.2\%$ and (b) $-3.5\% < R_{ee,s1} < +7.0\%$. These results are consistent with our experimental results as shown in Fig. 6.

The technique of dual synchronization could be applied for more than two chaotic oscillators. We speculate that the increase of the number of chaotic oscillators results in the limitation of parameter regions where separate synchroniza-

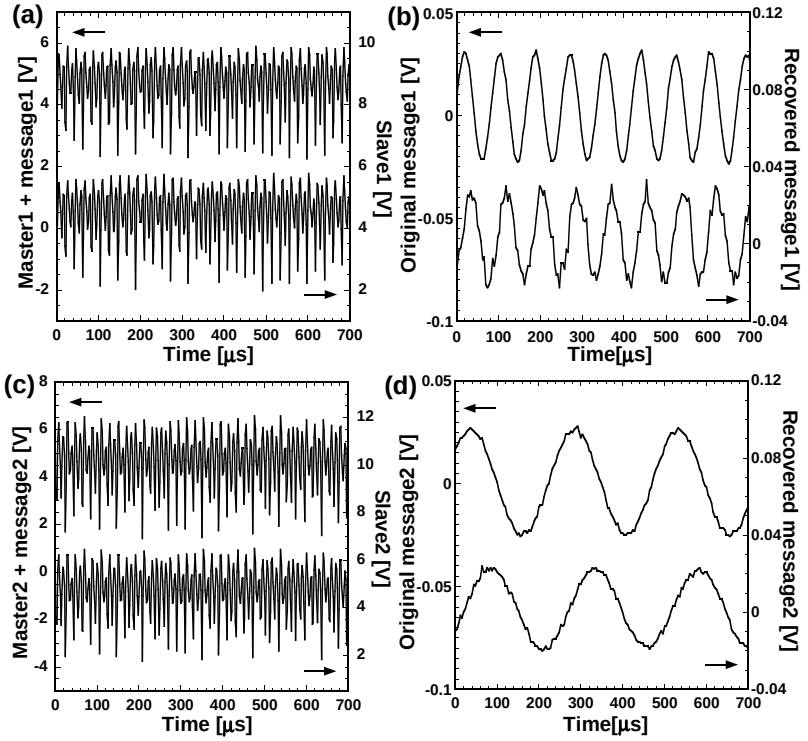

FIG. 12. Experimental demonstration of our communication scheme using dual synchronization of chaos. Temporal wave forms of (a) Master 1 + Message 1 and Slave 1, (b) the original Message 1 and the recovered Message 1, (c) Master 2 + Message 2 and Slave 2, and (d) the original Message 2 and the recovered Message 2.

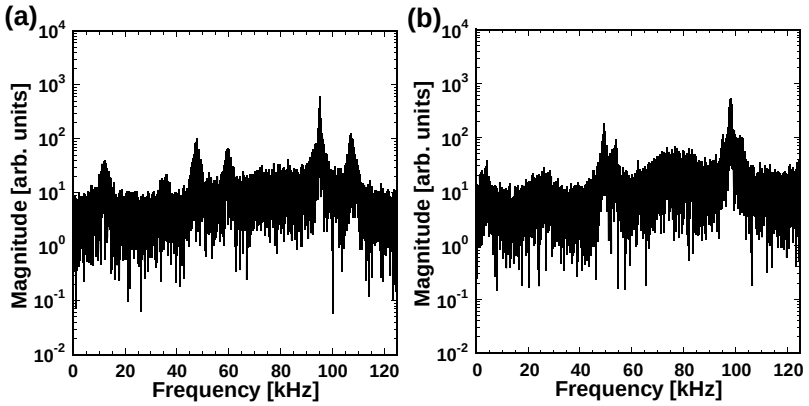

FIG. 13. rf spectra obtained from the temporal wave forms of (a) Master 1 + Message 1 and (b) Master 2 + Message 2 shown in Figs. 12(a) and 12(c).

tion is achieved. The influence of the number of chaotic oscillators upon the accuracy of separate synchronization will be investigated in our future work.

IV. APPLICATIONS FOR COMMUNICATIONS

We experimentally demonstrate a communication scheme by using dual synchronization of chaos in the Colpitts oscillators. Our scheme is shown in Fig. 10. A message is externally added on each chaotic carrier of M1 or M2 independently. Each pair has a transmission line to deliver the mixed signal of the chaos and message components. In order to achieve dual synchronization of chaos, we also have additional transmission line for the mixture of two chaotic wave forms between M1 and M2. Thus there are three transmission channels in our scheme. In the receivers, we can extract the corresponding chaotic wave form from the sum of two chaotic wave forms by using the technique of dual synchronization of chaos. Since there is no message signal on the synchronization signal $V_{m1}+V_{m2}$, our scheme allows to maintain high accuracy of dual synchronization of chaos. The idea of the separation of synchronization signal from the transmission signal with a message has been proposed in Ref. [24]. Although all the transmission channels are accessible by eavesdroppers, the original messages cannot be decoded without separating the two chaotic wave forms between M1 and M2. Random message signals must be used in this scheme in order to avoid the detection of the message by eavesdroppers.

Figure 11 shows the circuit diagram for the implementation of our communication scheme using dual synchronization of chaos. Each message is individually added to each chaotic wave form by an inverting adder circuit. The mixed signal is transmitted to the corresponding receiver. Two original chaotic signals in the two master oscillators are also added and sent to the two slave oscillators for dual synchronization. There is no recognizable delay between the mixed

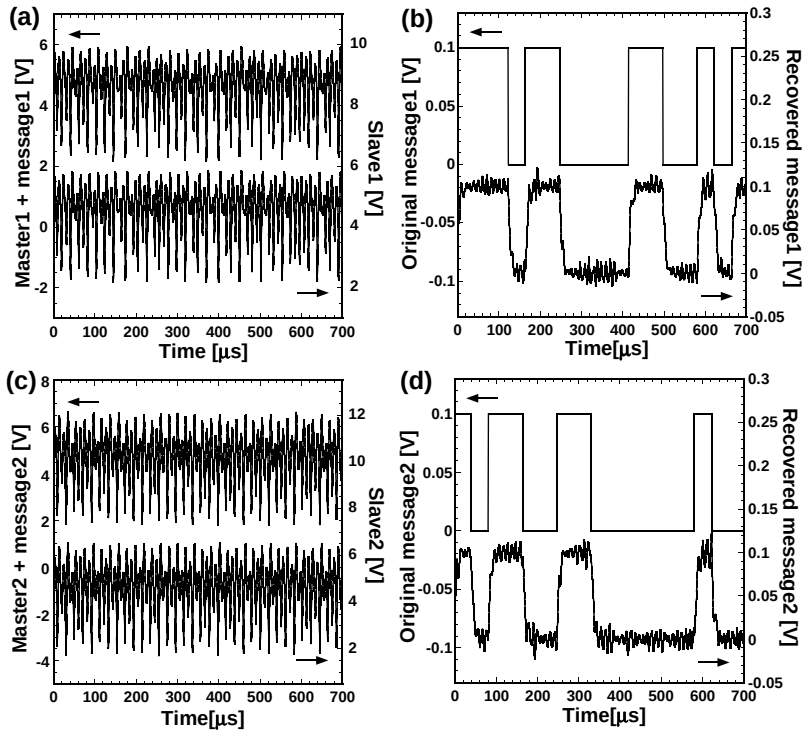

FIG. 14. Numerical demonstration of our communication scheme using dual synchronization of chaos. Temporal wave forms of (a) Master 1 + Message 1 and Slave 1, (b) the original Message 1 and the recovered Message 1, (c) Master 2 + Message 2 and Slave 2, and (d) the original Message 2 and the recovered Message 2.

chaotic signal and the transmission signals carrying the messages, because the oscillation frequency of chaotic signals is relatively slow around 95 kHz. In each receiver, the message can be subtracted from the transmission signal by using a synchronized chaotic wave form obtained from the procedure of dual synchronization. The subtracted message signal is applied to a low pass filter, and the original message can be recovered.

We use two different sinusoidal wave forms as message signals for simple demonstration in experiments. The frequencies of the two messages for M1 and M2 are set to 12 and 4 kHz, respectively. The depths of the modulations are set small enough to 0.013 and 0.010 for M1 and M2, respectively, so that the message components cannot appear on the chaotic carriers. The cutoff frequencies of the low pass filters at the final stage of the message recovery are set to 15 and 5 kHz, respectively. Figure 12 shows the temporal wave forms of transmission signals (chaos and message), synchronized signals in the slave lasers, and message components, obtained by experiment. It is difficult to distinguish the message component from the transmission signal as shown in Figs. 12(a) and 12(c). However, we can successfully recover two independent message components as shown in Figs. 12(b) and 12(d) after subtracting the chaotic wave forms from the transmission signal and passing them into the low pass filters. The distortion of the recovered signals is very small. Figure 13 shows the rf spectra of the temporal wave forms for the transmission signal (chaos and message) shown in Figs. 12(a) and 12(c). There is no sharp peak corresponding to the message frequency on the rf spectra. Since the message components are very small, it is difficult to find the message components without achieving dual synchronization of chaos.

We also numerically confirm our communication scheme. The configuration is the same as shown in Fig. 10. We use random digital sequences as messages in our simulation. The depths of the messages are set to 0.10 and the fundamental frequencies of the random square waves are set to 24 kHz for both M1 and M2. The low pass filters with the cutoff frequency of 30 kHz are used for message recovery. Figure 14 shows the temporal wave forms of transmission signals (chaos and message), synchronized signals in the slave lasers, and message components, obtained by numerical calculation. Although message components do not appear in the temporal wave forms of the transmission signal, we can clearly observe the random digital sequences for both of the messages by subtracting the synchronized signals, which are obtained by dual synchronization of chaos. The binary bits can be judged from the recovered message signals according to a certain threshold value even though the recovered messages contain small portions of chaotic fluctuations. Therefore, we have experimentally and numerically demonstrated our communication scheme using dual synchronization of chaos.

Our communication scheme is based on multiple transmission channels in order to avoid the distortion of synchronization signal when messages are added to chaotic signals. As proposed in Ref. [25–28], when a message signal is added in a chaotic system with a time-delayed feedback loop, synchronization of chaos can be maintained even in the presence of the message component on the chaotic signal. In such a time-delayed feedback system, dual synchronization of chaos could have a potential to achieve multiplex communications. The multiplex communications using dual synchronization of chaos will be our future work.

V. CONCLUSION

We have demonstrated the dual synchronization of chaos in two pairs of one-way coupled Colpitts electronic oscillators by both experiment and numerical simulation. We use the cross coupling method, where the difference in voltage between the sum of two master oscillators and one slave oscillator is injected into the other slave oscillator as an electrical current, for dual synchronization of chaos. We have investigated the regions for achieving dual synchronization of chaos when one of the internal parameters is mismatched between the master and slave oscillators. We numerically obtain a similar curve for the accuracy of synchronization to that obtained from our experiments. We have also demonstrated our communication scheme using dual synchronization of chaos. The technique of dual synchronization could be applied for higher-frequency chaotic electronic circuits and chaotic lasers oscillating at gigahertz frequencies.

ACKNOWLEDGMENTS

We acknowledge Peter Davis for helpful discussions. M.K. acknowledges Kinashi Denki Co. Ltd. for financial support. This work was financially supported by The Sumitomo Foundation, The Telecommunications Advancement Foundation, the Sasakawa Scientific Research Grant from The Japan Science Society, The Promotion and Mutual Aid Corporation for Private Schools of Japan, and Grant-in-Aid for Encouragement of Young Scientists from the Japan Society for the Promotion of Science.

[1] L.M. Pecora and T.L. Carroll, Phys. Rev. Lett. **64**, 821 (1990).
[2] K.M. Cuomo and A.V. Oppenheim, Phys. Rev. Lett. **71**, 65 (1993).
[3] M.P. Kennedy, R. Rovatti, and G. Setti, *Chaotic Electronics in Telecommunications* (CRC Press, Boca Raton, 2000).
[4] K. Yoshimura, Phys. Rev. E **60**, 1648 (1999).
[5] L.S. Tsimring and M.M. Sushchik, Phys. Lett. A **213**, 155 (1996).
[6] Y. Liu and P. Davis, Phys. Rev. E **61**, R2176 (2000).
[7] M.P. Kennedy, IEEE Trans. Circuits Syst., I: Fundam. Theory Appl. **41**, 771 (1994).
[8] G.M. Maggio, O. De Feo, and M.P. Kennedy, IEEE Trans. Circuits Syst., I: Fundam. Theory Appl., **46**, 1118 (1999).
[9] O. De Feo, G.M. Maggio, and M.P. Kennedy, Int. J. Bifurca-

tion Chaos Appl. Sci. Eng., **10**, 935 (2000).
[10] G.M. Maggio, M. di Bernardo, and M.P. Kennedy, IEEE Trans. Circuits Syst., I: Fundam. Theory Appl., **47**, 1160 (2000).
[11] F. O'Cairbre, G.M. Maggio, and M.P. Kennedy, Int. J. Bifurcation Chaos Appl. Sci. Eng., **7**, 2561 (1997).
[12] G. Sarafian and B.Z. Kaplan, IEEE Trans. Circuits Syst., I: Fundam. Theory Appl., **42**, 373 (1995).
[13] M.P. Kennedy, IEEE Trans. Circuits Syst., I: Fundam. Theory Appl., **42**, 376 (1995).
[14] W.W. Chai and L.O. Chua, Int. J. Bifurcation Chaos Appl. Sci. Eng., **5**, 895 (1995).
[15] Z. Galias, C.A. Murphy, M.P. Kennedy, and M.J. Ogorzalek, Chaos, Solitons Fractals **8**, 1471 (1997).
[16] K. Myneni, T.A. Barr, N.J. Corron, and S.D. Pethel, Phys. Rev. Lett. **83**, 2175 (1999).
[17] A. Tamasevicius, G. Mykolaitis, S. Bumeliene, A. Cenys, A.N. Anagnostopoulos, and E. Lindberg, Electron. Lett. **37**, 549 (2001).
[18] V. Rubezic and R. Ostojic, Proc. IEEE ICECS'99 **1**, 153 (1999).
[19] C. Ababei and R. Marculescu, Proc. IEEE APCCAS **2000**, 30 (2000).
[20] S. Moro and T. Matsumoto, Proc. NOLTA 2001 **1**, 167 (2001).
[21] A. Uchida, K. Takahashi, M. Kawano, and S. Yoshimori, IEICE Trans. Fundamentals **E85-A**, 2072 (2002).
[22] A. Uchida, T. Ogawa, M. Shinozuka, and F. Kannari, Phys. Rev. E **62**, 1960 (2000).
[23] A. Uchida, T. Matsuura, S. Kinugawa, and S. Yoshimori, Phys. Rev. E **65**, 066212 (2002).
[24] W.L. Ditto and L.M. Pecora, Sci. Am. **269**(2), 62 (1993).
[25] A.R. Volkovskii and N. Rulkov, Tech. Phys. Lett. **19**, 97 (1993).
[26] H.D.I. Abarbanel and M. Kennel, Phys. Rev. Lett. **80**, 3153 (1998).
[27] G.D. VanWiggeren and R. Roy, Science **279**, 1198 (1998).
[28] J.-P. Goedgebuer, L. Larger, and H. Porte, Phys. Rev. Lett. **80**, 2249 (1998).